Journal Pre-proof

PROTHYMOSIN A GENE TRANSDUCTION ATTENUATED CARDIOPULMONARY REMODELING AND MORTALITY IN FLOW-INDUCED PULMONARY HYPERTENSION RAT MODEL

Jun-Neng Roan MD, PhD , Chih-Hsin Hsu MD, PhD , Shih-Yuan Fang MD , Meng-Shuan Chiu MSc , Chao-Liang Wu PhD , Ai-Li Shiau PhD , Chen-Fuh Lam MD, PhD

PII: S1053-2498(20)31580-1
DOI: https://doi.org/10.1016/j.healun.2020.05.017
Reference: HEALUN 7181

To appear in: *Journal of Heart and Lung Transplantation*

Please cite this article as: Jun-Neng Roan MD, PhD , Chih-Hsin Hsu MD, PhD , Shih-Yuan Fang MD , Meng-Shuan Chiu MSc , Chao-Liang Wu PhD , Ai-Li Shiau PhD , Chen-Fuh Lam MD, PhD , PROTHYMOSIN A GENE TRANSDUCTION ATTENUATED CARDIOPULMONARY REMODELING AND MORTALITY IN FLOW-INDUCED PULMONARY HYPERTENSION RAT MODEL, *Journal of Heart and Lung Transplantation* (2020), doi: https://doi.org/10.1016/j.healun.2020.05.017

PROTHYMOSIN A GENE TRANSDUCTION ATTENUATED CARDIOPULMONARY REMODELING AND MORTALITY IN FLOW-INDUCED PULMONARY HYPERTENSION RAT MODEL

Jun-Neng Roan, MD, PhD[1,2], Chih-Hsin Hsu, MD, PhD[3], Shih-Yuan Fang, MD[4], Meng-Shuan Chiu, MSc[4], Chao-Liang Wu, PhD[5,6], Ai-Li Shiau, PhD[7†], and Chen-Fuh Lam, MD, PhD[8*†]

[1]Division of Cardiovascular Surgery, Department of Surgery, National Cheng Kung University Hospital, College of Medicine, National Cheng Kung University, Tainan, Taiwan [2]Medical Device Innovation Center, National Cheng Kung University Hospital, College of Medicine, National Cheng Kung University, Tainan, Taiwan

[3]Division of Cardiology, Department of Internal Medicine, College of Medicine, National Cheng Kung University, Taiwan

[4]Department of Anesthesiology, National Cheng Kung University Hospital, College of Medicine, National Cheng Kung University, Tainan, Taiwan

[5]Institute of Basic Medical Sciences, College of Medicine, National Cheng Kung University, Tainan, Taiwan

[6]Department of Biochemistry, College of Medicine, National Cheng Kung University, Tainan, Taiwan

[7]Department of Microbiology and Immunology, College of Medicine, National Cheng Kung University, Tainan, Taiwan

[8]Department of Anesthesiology, E-Da Hospital/I-Shou University, 1 Yida Road, Yanchao District, Kaohsiung City 824, Taiwan

[†]These authors contributed equally to the study.

*Corresponding author: ed110208@edah.org.tw

Grant Support: This work was supported by grants from E-Da Hospital/I-Shou University (Grant number: NCKUEDA10815 to JNR) and from the National Science Council of Taiwan (Grant number:

MOST 107-2314-B-006-077 to JNR; Grant number: MOST 105-2314-B-303-007-MY2 to CFL).

Running Title: Prothymosin α in Flow-induced Pulmonary Hypertension

Word count: 245/250 words in Abstract, and 2993/3,000 words in the manuscript.

This manuscript contains 7 figures/1 table, and 29/30 references

Abstract

Background. Prothymosin α (*ProT*) is a cell survival gene which modulates oxidative stress and transforming growth factor (TGF)-β signaling. We hypothesized that the delivery of the prothymosin α (ProT) cDNA gene in rats could protect against right heart dysfunction secondary to pulmonary hypertension (PH) induced by left-to-right shunt.

Methods. A two-hit rat model of flow-induced PH was used, and a single intravenous injection of adenoviral vectors (2×10^9 plaque forming unit) carrying *ProT* or luciferase gene was administered. The animals were euthanized 21 days after gene delivery to assess cardiopulmonary function, serum biochemistry, pulmonary artery (PA) and vasomotor reactivity. Immunohistology and immunoblotting of PA tissues was also performed.

Results. *ProT* transduction significantly reduced PA pressure, right ventricle muscle mass, and wall stress, thereby improving the overall survival of the treated rat. Increased production of ProT through gene therapy preserved both the smooth muscle myosin heavy chain-II and α-smooth muscle actin, while counteracting the abundance of TGF-β in PA. Protein abundances of phosphorylated p47-phox, heme oxygenase-1, caspase-3, inducible nitric oxide synthase, cyclo-oxygenase 2, and monocyte chemoattractant protein-1 in PA tissues were reduced. ProT also preserved microRNA-223, thereby suppressing the abundance of poly(ADP-ribose)polymerase-1, which is independent of hypoxia inducible factor-1α signaling.

Conclusions. *ProT* gene transduction improved PA function by reducing oxidative stress, attenuating inflammation, and preserving the contractile phenotype of vascular smooth muscle cells. The modification of microRNA–223-associated downstream signaling through *ProT* transduction may play an important role in mitigating cardiopulmonary remodeling in flow-induced PH.

Key words: flow-induced pulmonary hypertension; Prothymosin α; microRNA-223

Introduction

Patients with intracardiac left-to-right shunt, such as those with atrial septal defects, have a 3–5% increased risk of developing pulmonary arterial hypertension (PAH) if left untreated.[1] Despite the availability of modern medications for PAH, the procedure for intracardiac left-to-right shunt continues to carry an increased risk.[2, 3] In addition, the repair of congenital defects alone does not warrant regression of pulmonary hypertension (PH).[4] Advances in targeted medical therapy or its combination with the closure of left-to-right shunt improves the survival of PAH patients, although the disease remains fatal.[5, 6] Therefore, the development of effective therapies for PAH remains an unmet medical need.[5]

The polypeptide prothymosin α (ProT) contains 109–113 amino acids and is highly conserved in eukaryotes.[7] Previously, we showed that *ProT* gene transfer using adenoviral vectors preserved nitric oxide (NO)-mediated signaling and enhanced the expression of heme oxygenase (HO)-1 in aorta tissue of Apolipoprotein $E^{-/-}$ mice.[8] As a multifunctional protein, ProT is reported to be involved in cell survival and differentiation.[9] In addition, our previous study, employing a pulmonary emphysema mouse model, revealed that ProT is involved in the inhibition of transforming growth factor (TGF)-β signaling.[10] TGF-β is an important mediator involved in modulating the differentiation of mature vascular smooth muscle cells (VSMC) in PAH and pulmonary fibrosis.[11, 12] However, the potential role of ProT has yet to be determined in PAH.

In this study, we hypothesized that the administration of *ProT* through gene delivery might protect rats against right heart failure caused by left-to-right shunt-induced PH. Moreover, considering that pre-clinical gene therapy and epigenetic control studies using micro-ribonucleic acids (RNAs) showed promising therapeutic effects,[5, 11] we sought to elucidate the role of *ProT* transduction therapy in a flow-induced PH rat model.

Materials and Methods

Animal model

Age-matched, young male Sprague–Dawley rats, weighing 200–250 g, were kept in an animal house with a 12h/12h light/dark cycle. They were provided a standard chow diet and water *ad libitum*. All procedures were performed in accordance with the guidelines of the Animal Care and Use Committee of National Cheng Kung University, Taiwan. Aortocaval fistula, or left-to-right shunt, was induced as described previously.[13] On day (*d*)21 post-treatment, the rats were euthanized with pentobarbital sodium (250 mg/kg *ip*).

Induction of modified flow-induced pulmonary vascular change in rats

A single dose of monocrotaline (Oakwood Products, Inc., USA; 60 mg/kg) was subcutaneously injected to each rat. Aortocaval fistula surgery was performed after 7 days.[13, 14] The animals would develop symptoms of dyspnea and heart failure within 4 weeks after the monocrotaline injection as described previously.[13, 14]

Construction of adenoviral vectors

Detailed information is described in supplementary material. In brief, to generate a recombinant adenovirus, the adenoviral transfer vector pAd5L-*ProT* and the adenoviral type 5 genomic vector were cotransfected into 293 cells by calcium phosphate precipitation. Recombinant adenovirus encoding firefly luciferase, designated Ad*Luc*, was used as the control virus.[8, 15, 16]

Treatment protocol

Rats were randomly allocated into two groups, i.e., PH group, treated with Ad*Luc*, and PH+*ProT* group, treated with Ad*ProT*, *d*21 after the induction of aortocaval fistula (**Figure S1)**. A single shot of the adenoviral vectors (2 x 10^9 plaque forming unit) in 50 μL phosphate-buffered saline (PBS) was administered to each rat through the internal jugular vein.[8] The dose was determined from our previous atherosclerosis study.[8] Another group of rats, the sham group, were composed of normal rats that received a single injection of PBS.

Hemodynamic measurements and vasomotor function assessment

Echocardiography

Transthoracic echocardiography was performed in anesthetized rats before euthanasia using

ACUSON X300 Premium Edition (Siemens Ultrasound System, USA) with a 9.2 MHz probe (P9-4 phased array transducer, Siemens Medical Solutions, USA).[13, 17]

Invasive hemodynamic assessment

Pressure measurements of the right ventricle (RV) and left ventricle (LV) were performed under anesthesia using isoflurane (2–3% v/v in oxygen) as previously described.[13] The RV end-systolic pressure (RVESP) was used as a surrogate indicator of pulmonary artery (PA) pressure.[13, 18] The rats were euthanized after invasive hemodynamic measurements, and their hearts and lungs were removed *en bloc* for analysis as described previously.[19]

RV morphological analysis

The hearts of the rats were dissected to isolate the free wall of the RV from the LV and septum. The RV/LV+septum muscle ratio was designated as the index (Fulton index) of RV hypertrophy.[13]

Quantitative analysis of serum biochemistry

Blood samples were collected before euthanasia for further analysis. Blood glucose, triglyceride, cholesterol, aspartate transaminase (AST), alanine transaminase (ALT), blood urea nitrogen (BUN), and creatinine levels were analyzed using colorimetric assays (ADVIA 1800 Chemistry System, Siemens).[20] Enzyme-linked immunosorbent assay (ELISA) detection kits were used according to the manufacturer's instructions to measure serum brain natriuretic peptide (BNP; AssayMax®, Assaypro LLC, USA) and ProT (FineTest®, Wuhan Fine BiotechCo.,Ltd., China) concentrations.

Pulmonary artery and tissue preparation

Vasomotor reactivity

The main PA rings (~3 mm in length) were mounted on organ chambers containing 25 mL of Krebs solution as previously described.[21]

Histology of pulmonary arteries and arterioles

The detailed processing of PA and lung tissue samples are described in the supplementary material. For the main PA tissues, the media thickness ratio, defined as media thickness divided by the thickness of the whole artery, was used to evaluate medial hyperplasia. The intra-acinar pulmonary arterioles, defined as vessels with diameters < 150 μm,[22] were also evaluated to determine the medial

thickness area as previously described.[13]

Immunohistochemistry and in situ hybridization

Immunohistochemistry (IHC) was performed in the prepared tissue sections using the Bond-Max Automated IHC stainer (Leica Biosystems Newcastle Ltd., Australia). The sections were incubated with rabbit anti-ProT (1:200 dilution) at 25 °C for 30 min and counterstained with hematoxylin. Tissue *in situ* hybridization (ISH) was stained with microRNA (miR)-223-3p (sequence 5'-ggg gta ttt gac aaa ctg aca-3') probe (BioTnA, Kaohsiung, Taiwan), and the expression levels were determined using the Biospot ISH detection kit (TASH01D, BioTnA, Kaohsiung, Taiwan). Quantification was performed using ImageJ software (National Institutes of Health, Rockville, Md).

Western blot analysis

Soluble protein (50 μg) extracted from PA were prepared for incubation with the appropriate primary antibodies as previously described.[23] Detailed methods for immunoblotting analysis are described in supplementary materials.

Statistical analysis

Unless specified, data are presented as the mean ± standard deviation (SD). Detailed statistical methods are described in supplementary materials. Statistical significance was accepted at $P < 0.05$. All statistical analyses were performed using the SigmaPlot 14.0 (Systat Software Inc., San Jose, CA).

Results

ProT gene transduction reduces right ventricular wall stress and improves overall survival.

The overall survival of PH rats on *d*21 after treatment was 30.77 ± 3.70%, whereas that with the *ProT* gene transduction was significantly improved to 64.71 ± 2.94% ($P = 0.04$; **Figure 1A)**. RV hypertrophy was significantly observed using Fulton index in PH rats. Meanwhile, P*roT* gene transduction attenuated the RV muscle mass in the PH group (**Figure 1B**). Consistent with these morphological findings, serum BNP levels were reduced (**Figure 1C)**.

Serum* ProT*, biochemistry, and body weight changes after gene transduction.

There were no significant changes in PH rats in terms of serum levels of ProT, which were significantly elevated on *d*21 after gene transduction ($P < 0.001$, **Figure S2**). A significant regain of body weight was found in the treatment group (P = 0.004). Among PH rats, a significant elevation in serum BUN and AST levels was observed, and both were significantly recovered in the treatment group ($P < 0.001$ and $P = 0.002$, respectively; **Table S1**).

ProT gene transduction attenuates the remodeling of PA and RV. Echocardiography showed the remodeling of the main PA due to the left-to-right shunt in the PH group (**Table 1 and Figure S3)**. Meanwhile, transduction of the *ProT* gene attenuated the dilated remodeling and the peak blood flow velocity of PA ($P < 0.001$). Moreover, ProT reversed the dilatation in the RV, along with a decreased peak flow velocity across the tricuspid valve ($P < 0.001$ and $P = 0.002$, respectively). There were no statistically significant changes in the left ventricular ejection fraction after treatment.

Invasive hemodynamic data showed no statistically significant differences in heart rate, left ventricle end-systolic pressure (LVESP), or left and right ventricle end-diastolic pressures (LVEDP, RVEDP) on the day of euthanasia (**Table S2)**. A significant elevation in RVESP was found in the control group (71.21 ± 13.2 mmHg vs 21.44 ± 7.41 mmHg in sham; $P < 0.001$). Transduction of *ProT* reduced RVESP (54.16 ± 8.13 mmHg vs 71.21 ± 13.2 mmHg; $P = 0.008$). Since the pulmonary arterial pressure correlates with systemic pressure;[24] to avoid reading interference we included the ratio of the mean right ventricular pressure and the mean left ventricular pressure (mRV/mLV) to show the degree of PH. This ratio was significantly reduced in the treatment group (**Table S2**; $P < 0.001$).

ProT *preserves the endothelial function and attenuates pathological contractions in PA of PH rats.*

The contractions to potassium chloride (KCl, 40 mM) and phenylephrine (PE, 10^{-9}–10^{-5} M) were significantly increased in PH rats (**Figure 2A)**, whereas *ProT* transduction significantly attenuated the maximum non-selective (to KCl) and selective (to PE, α1-agonist) contractions (**Figure 2A, 2B)**. There was a decrease in tension responses to PE in the PA of the ProT group, **Figure 2B**. However, the concentration for 50% of the maximal effect of PE was not significantly changed (**Figure 2C)**. Endothelium-dependent relaxation to acetylcholine were significantly impaired in PH rats, and the relaxation response curve shifted to the left in the treatment group at concentrations greater than 10^{-6}M ($P < 0.05$; **Figure 2D**).

ProT *reduces the medial thickness in PA and arterioles of PH rats.*

There was a significant media thickening of the major PA ($P = 0.045$) and intra-acinar arterioles of PH animals ($P < 0.001$; **Figure 3)**. Gene transduction with Pro*T* showed a significantly reduced thickness in the media layer of PA ($P = 0.034$) and arterioles ($P < 0.001$).

ProT *reverses de-differentiation of VSMC in PA.*

Immunoblotting analysis of PA tissues showed that the abundance of proteins representative of the contractile phenotype in VSMC, including α- smooth muscle actin (SMA) and smooth muscle myosin heavy chain (SM-MHC) class II, were reduced in PH rats (**Figure 4)**. In contrast, increased matrix metalloproteinase (MMP)-2 protein abundance was observed in PH animals. *ProT* transduction preserved the contractile protein abundance, however, reduced the expression of their counterpart protein. The mobilization of TGF-β, which enhanced VSMC de-differentiation, was observed in PH animals, while there was a significant reduction in TGF-β in PA tissues of the treatment group (**Figure 4A** and **4E).**

ProT *exhibits anti-oxidative and anti-inflammatory responses in PA tissue.* Oxidative stress associated protein abundances of phosphorylated (p)-p47-phox, HO-1, and Kelch-like ECH-associated protein (KEAP)-1, along with caspase 3 were significantly increased in the PA of PH rats, however, were reduced in the treatment group (**Figure 5)**. There was an increased protein abundance of endothelial nitric oxide synthase (eNOS) in PH animals partly due to the persistently high shear stress to PA from the left-to-right shunt (**Figure 6A and 6B)**. Immunoblotting analysis of

PA tissues from PH rats showed enhanced levels of inflammatory marker proteins, including inducible nitric oxide synthase (iNOS), cyclooxygenase (COX)-2, and monocyte chemoattractant protein (MCP)-1, which were suppressed after transduction with the *ProT* gene (**Figure 6)**.

ProT *reduces poly(ADP-ribose)polymerase (PARP)-1 in PA tissues, which is independent of hypoxia inducible factor (HIF)-1α signaling.*

Increased ProT expression was observed in PA tissues, which was associated with PH (Figure 7A). Transduction with *ProT* further induced a significant increase in ProT tissue expression ($P = 0.006$; **Figure 7A and B)**. Meanwhile, the expression of miR-223 was detected in PA tissues of sham rats **(Figure 7A and C)**, and a significant reduction in miR-223 expression was found in PH animals. In contrast, treatment with *ProT* retained miR-223 expression ($P < 0.001$). Immunoblotting analysis of PA tissues of PH rats showed increased protein abundance of PARP-1, which was reduced in the treatment group (**Figure 7D**). HIF-1α, which enhances PARP-1 expression through the inhibition of miR-223, was significantly increased in PH animals (**Figure 7D and E**). However, ProT did not attenuate the abundances of HIF-1α in PA tissues.

Discussion

Our study showed that intravenous *ProT* gene delivery reduced PA pressure and reversed hypertrophic remodeling in both PA and RV in flow-induced PH rats, while significantly improving survival rates. Among the five groups of PH in the World Health Organization's classification, flow-induced PH belongs to group 1. Although numerous studies have investigated the pathogenesis of group 1 PAH, only a few have focused on the flow-induced (or congenital heart disease) subgroup. In our previous report, this clinically relevant "two-hit" PH model was found to induce the de-differentiation of VSMCs, significantly contributing to the flow-induced cardiovascular pathology.[13] Transduction of *ProT* attenuated VSMC de-differentiation, thereby reversing PA remodeling. Histological findings confirmed a significant reduction in medial thickening of both major and resistant PA. Overall, our findings demonstrate that ProT may be a potential therapeutic marker gene for the treatment of flow-induced PH.

Oxidative stress in PA might result in a vicious cycle causing induced endothelial dysfunction.[25]. In the current study, vasomotor functional analysis showed that treatment with the *ProT* gene partly preserved endothelial function. Specifically, contraction responses to α-agonist and KCl were significantly normalized in PA transduced with *ProT* gene therapy. Therefore, we speculated that the reverse-remodeling of the PA medial layer, rather than preservation of the endothelial function, is the major mechanism responsible for relieving PH.

De-differentiated VSMCs, characterized by proliferation, migration, and loss of contractile proteins, play a pivotal role in PA remodeling in PAH.[13, 26] TGF-β was identified to play an important role in directing VSMCs toward differentiation in major vessels.[12] Consistent with previous studies in PAH involving PA from the human tissue and animal models,[11, 12, 26] we also observed up-regulation of TGF-β. Interestingly, the overexpression of TGF-β was found in conjunction with proliferation of de-differentiated PA smooth muscle cells both *in vitro* and *in vivo*.[12, 26] Zabini D. et al. proposed that the down-regulation of SMAD3, followed by disinhibition of post-translational signal responses under chronic stress from PH, could contribute to these conflicting findings.[26] They further reported an increase in α-SMA expression in differentiated VSMCs under prolonged mobilization of TGF-β in

lung tissues of PAH patients and in both pre-clinical rat models of monocrotaline- and hypoxia-induced PH.[26] However, α-SMA is non-specific for VSMCs and could be identified in other lung tissue cell types, such as endothelial cells and fibroblasts under pathological stress or TGF-β stimulation.[27] Therefore, we investigated PA rather than lung tissues in this study, and observed down-regulation of contractile proteins, including α-SMA and SM-MHC II. The up-regulation of MMP2 also supports VSMC de-differentiation in our flow-induced PH model. The observed reduction in TGF-β abundances in the ProT group could be a consequence of the attenuated PH after treatment. Therefore, we speculate that oxidative stress overload and inflammation responses, rather than TGF-β mobilization, equally contribute to the remodeling of PA in flow-induced PH. However, we were unable to exclude the possibility of differences in pathophysiology between flow-induced PH and other PH models simulating clinical group 1 PH category.

Young L. et al showed in transgenic mice that overexpression of miR-223 induces hypertrophy of cardiomyocytes.[28] Our unpublished data involving a transgenic mice model and emphysema patients showed that ProT could enhance miR-223 expression in pulmonary tissues. Moreover, Meloche J. et al reported that the activation of reactive oxygen species inhibited miR-223 through HIF-1α–mediated signaling.[29] The expression of PARP-1, originally inhibited by miR-223, was up-regulated, thereby inducing the de-differentiation of VSMCs *in vitro*.[29] Our study showed that HIF-1α was activated in the PA of PH rats, with and without *ProT* delivery. We would therefore expect a suppressed miR-223 expression in both groups. However, miR-223 was up-regulated, whereas PARP-1 was downregulated in the treatment group. In addition, inflammatory responses were inhibited, which is consistent with the down-regulation of PARP-1 after *ProT* transduction.[30] Overall, we propose that responsive ProT protein mobilization failed to attenuate cardiopulmonary remodeling in flow-induced PH. Gene therapy significantly increased ProT expression, which inhibited PARP-1 through the mobilization of miR-223 in PA tissues. Such a mechanism may be independent of HIF-1α up-regulation and may contribute to the phenotype switching of VSMC toward the differentiated status.

Certain limitations are noted regarding extrapolating the results of this study in flow-induced PH. For instance, although this two-hit rat model mimicked human subjects with PAH,[13, 14] flow-induced

PAH in humans is induced primarily by congenital heart diseases, which have a different pathophysiology from this adolescent rat model.[13] In addition, we did not evaluate the long-term effects of gene delivery which is important as off-target biological responses, such as the formation of neoplasm in other replicative organs, remain a safety concern in gene therapy. The efficacy of gene delivery in the pulmonary vascular system using intravenous injection was also not assessed; therefore, the optimal dose of *ProT*-adenoviral vectors in different body sizes was not justified.

In summary, we showed that *ProT* gene delivery reduced oxidative stress, inhibited inflammation, and attenuated apoptosis in the pulmonary vasculature of flow-induced PH rats. The successful transduction of *ProT* through intravenous injection of AdProT vectors up-regulated miR-223 and downregulated PARP-1. Furthermore, restoration of VSMC from a synthetic to contractile phenotype was observed following treatment with *ProT* in PA, which reversed its remodeling; meanwhile attenuation of pulmonary pressure reduced RV afterload and attenuated RV remodeling. Most importantly, *ProT* gene therapy improved the overall survival of rats suffering from flow-induced PH. This study presents a potential target for gene therapy for RV failure secondary to flow-induced PH.

Acknowledgments

We would like to thank the histology technical support from Li-Tzung Biotechnology INC., Kaohsiung, Taiwan.

Conflict of Interest: The authors declare no conflict of interest.

Authors' Contribution: JNR, ALS, and CFL designed the study. JNR, CHH, SYF, and MSC performed the animal experiments. JNR, CHH, SYF, and MSC performed data collection and analysis. JNR, CLW, ALS, and CFL contributed to the statistical analysis and interpretation of data. JNR, CLW, ALS, and CFL contributed to drafting the manuscript. All authors have read and approved the final version of manuscript. ALS and CFL: Both authors contributed in this study equally.

References

1. Lammers AE, Bauer LJ, Diller GP, et al. Pulmonary hypertension after shunt closure in patients with simple congenital heart defects. Int J Cardiol 2020; S0167-5273:35865-6. doi: 10.1016/j.ijcard.2019.12.070.

2. Akagi T. Current concept of transcatheter closure of atrial septal defect in adults. J Cardiol 2015; 65:17-25.

3. Favoccia C, Constantine AH, Wort SJ and Dimopoulos K. Eisenmenger syndrome and other types of pulmonary arterial hypertension related to adult congenital heart disease. Expert Rev Cardiovasc Ther 2019; 17:449-59.

4. Kijima Y, Akagi T, Takaya Y, et al. Treat and repair strategy in patients with atrial septal defect and significant pulmonary arterial hypertension. Circ J 2015; 80:227-34.

5. Sitbon O, Gomberg-Maitland M, Granton J, et al. Clinical trial design and new therapies for pulmonary arterial hypertension. Eur Respir J 2019; 53:1801908.

6. Klinger JR, Elliott CG, Levine DJ, et al. Therapy for pulmonary arterial hypertension in adults: Update of the CHEST Guideline and Expert Panel Report. Chest 2019; 155:565-86.

7. Schmidt G and Werner D. Nucleotide sequence of the murine prothymosin alpha cDNA and its deduced primary and secondary protein structure. Biochim Biophys Acta 1991; 1088:442-4.

8. Chang MY, Yang YS, Tsai ML, et al. Adenovirus-mediated prothymosin alpha gene transfer inhibits the development of atherosclerosis in ApoE-deficient mice. Int J Biol Sci 2014; 10:358-66.

9. Jiang X, Kim H-E, Shu H, et al. Distinctive roles of PHAP proteins and prothymosin-α in a death regulatory pathway. Science. 2003; 299:223-6.

10. Humbert M, Guignabert C, Bonnet S, et al. Pathology and pathobiology of pulmonary hypertension: state of the art and research perspectives. Eur Respir J 2019; 53:1801887.

11. Rol N, Kurakula KB, Happe C, Bogaard HJ and Goumans MJ. TGF-beta and BMPR2 signaling in PAH: Two black sheep in one family. Int J Mol Sci 2018; 19:E2585.

12. Roan JN, Hsu CH, Fang SY, et al. Exendin-4 improves cardiovascular function and survival in flow-induced pulmonary hypertension. J Thorac Cardiovasc Surg 2018; 155:1661-9.

13. van Albada ME, Schoemaker RG, Kemna MS, Cromme-Dijkhuis AH, van Veghel R and Berger RMF. The role of increased pulmonary blood flow in pulmonary arterial hypertension. Eur Respir J 2005; 26:487-93.

14. McGrory WJ, Bautista DS and Graham FL. A simple technique for the rescue of early region I mutations into infectious human adenovirus type 5. Virology. 1988; 163:614-7.

15. Tai MH, Cheng H, Wu JP, et al. Gene transfer of glial cell line-derived neurotrophic factor promotes functional recovery following spinal cord contusion. Exp Neurol 2003;183: 508-15.

16. Roan JN, Fang SY, Chang SW, et al. Rosuvastatin improves vascular function of arteriovenous fistula in a diabetic rat model. J Vasc Surg 2012; 56:1381-9.

17. Koyama M, Furuhashi M, Ishimura S, et al. Reduction of endoplasmic reticulum stress by 4-phenylbutyric acid prevents the development of hypoxia-induced pulmonary arterial hypertension. Am J Physiol Heart Circ Physiol 2014; 306:H1314-23.

18. Lam CF, Roan JN, Lee CH, et al. Transplantation of endothelial progenitor cells improves pulmonary endothelial function and gas exchange in rabbits with endotoxin-induced acute lung injury. Anesth Analg 2011; 112:620-7.

19. Fang SY, Roan JN, Lin Y, et al. Rosuvastatin suppresses the oxidative response in the venous limb of an arteriovenous fistula and enhances the fistula blood flow in diabetic rats. J Vasc Res 2014; 51:81-9.

20. Roan JN, Yeh CY, Chiu WC, et al. Functional dilatation and medial remodeling of the renal artery in response to chronic increased blood flow. Kidney Blood Press Res 2011; 34:447-56.

21. Dahal BK, Kosanovic D, Kaulen C, et al. Involvement of mast cells in monocrotaline-induced pulmonary hypertension in rats. Respir Res 2011; 12:60.

22.. Lam CF, Liu YC, Tseng FL, et al. High-dose morphine impairs vascular endothelial function by increased production of superoxide anions. Anesthesiology 2007; 106:532-7.

23 Schubert SA, Mehaffey JH, Booth A, et al. Pulmonary-systemic pressure ratio correlates with morbidity in cardiac valve surgery. J Cardiothorac Vasc Anesth 2019; 33:677-82.

24. Lai YC, Potoka KC, Champion HC, Mora AL and Gladwin MT. Pulmonary arterial hypertension: the clinical syndrome. Circ Res 2014; 115:115-30.

25. Zabini D, Granton E, Hu Y, et al. Loss of SMAD3 promotes vascular remodeling in pulmonary arterial hypertension via MRTF disinhibition. Am J Respir Crit Care Med 2018; 197:244-60.

26. Kovacic JC, Dimmeler S, Harvey RP, et al. Endothelial to mesenchymal transition in cardiovascular disease: JACC State-of-the-Art Review. J Am Coll Cardiol 2019; 73:190-209.

27. Yang L, Li Y, Wang X, et al. Overexpression of miR-223 tips the balance of pro- and anti-hypertrophic signaling cascades toward physiologic cardiac hypertrophy. J Biol Chem 2016; 291:15700-13.

28. Meloche J, Guen ML, Potus F, et al. miR-223 reverses experimental pulmonary arterial hypertension. Am J Physiol Cell Physiol 2015; 309:C363-72.

29. Burkle A, Virag L. Poly(ADP-ribose): PARadigms and PARadoxes. Mol Aspects Med 2013; 34:1046-65.

Figure Legends

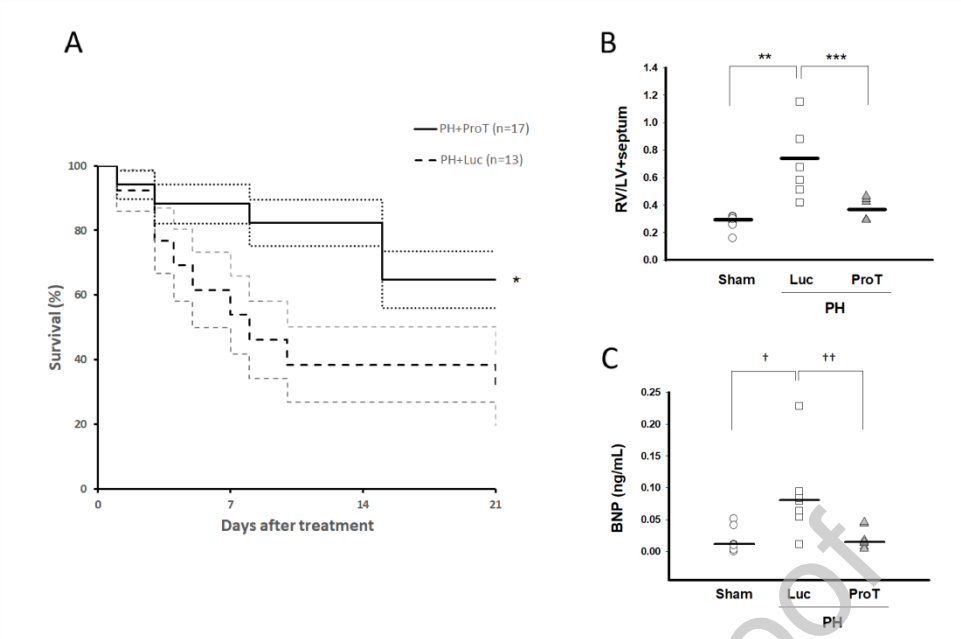

Figure 1. Survival and right ventricle (RV) hypertrophy indices**. A.** Kaplan–Meier survival of flow-induced pulmonary hypertension (PH) with luciferase (*Luc*) or prothymosin α (*ProT*) gene delivery. A total of 51 animals were used for survival analysis, and 30 of them survived to the time-point when animals were randomly assigned to receive treatment. **P* = 0.04. **B.** RV mass ratio (Fulton index; ***P* < 0.001 and ****P* = 0.002 using post Holm–Sidak method; n = 6–7 per group). **C.** Serum level of brain natriuretic peptide (BNP). †*P* = 0.01; ††*P* = 0.015 using post-hoc Dunnett's method; n = 7 per group. LV: left ventricle. The horizontal lines in **B.** and **C.** denote the median value.

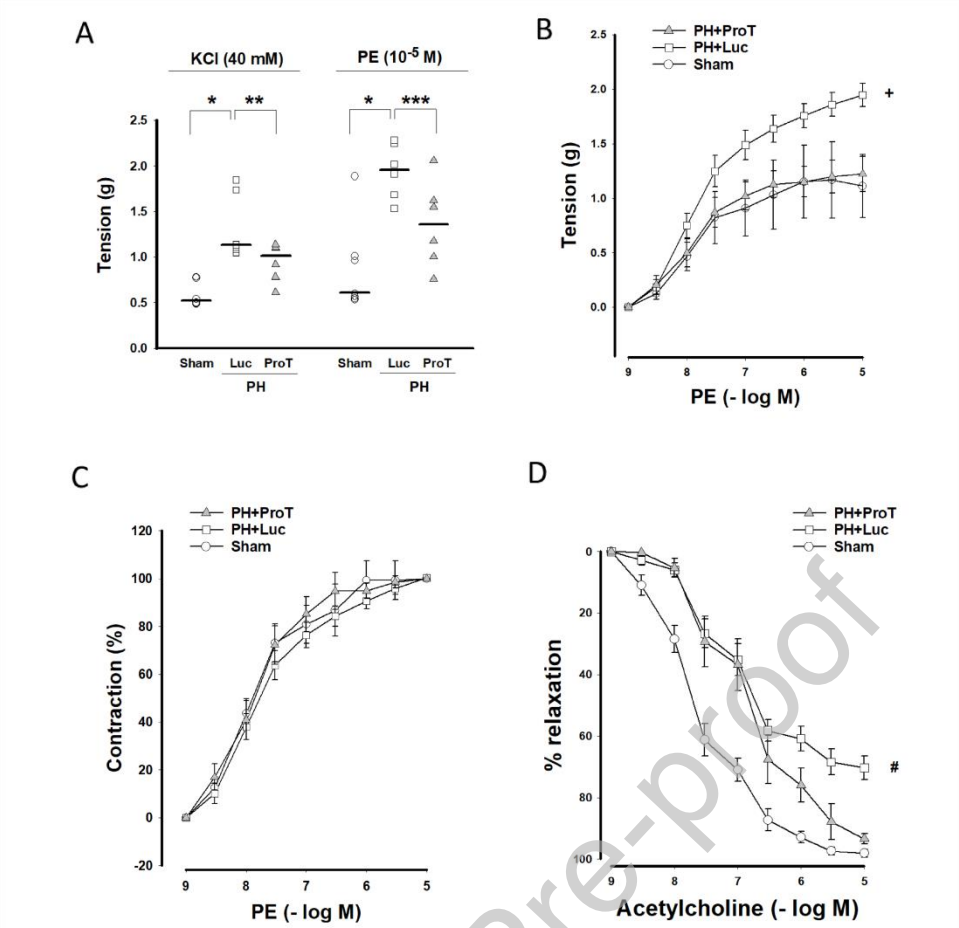

Figure 2. Vasomotor function analysis of pulmonary arteries (PAs) in pulmonary hypertension (PH) rats luciferase (Luc) or prothymosin α (*ProT*) gene therapy. **A**. Contraction responses to potassium chloride (KCl, 40mM) and phenylephrine (PE, 10^{-5} M). **B**. Contraction and **C**. Percentage contraction responses of PA to cumulative addition of phenylephrine (PE, 10^{-9}–10^{-5} M). **D**. Relaxation responses to cumulative addition of acetylcholine. Relaxation was obtained during contraction to EC_{60} (the concentration required to achieve 60% of maximum contraction) of PE. **P* = 0.003; ***P* < 0.001; ****P* = 0.018; $^{+}P < 0.001$ for PH+Luc vs PH+ProT and sham, respectively. $^{\#}P < 0.05$ for PH+Luc vs PH+ProT with concentration ≥ 10^{-6} M using post-hoc Holm–Sidak method. Data are presented as mean ± SE; n = 6–8 per group.

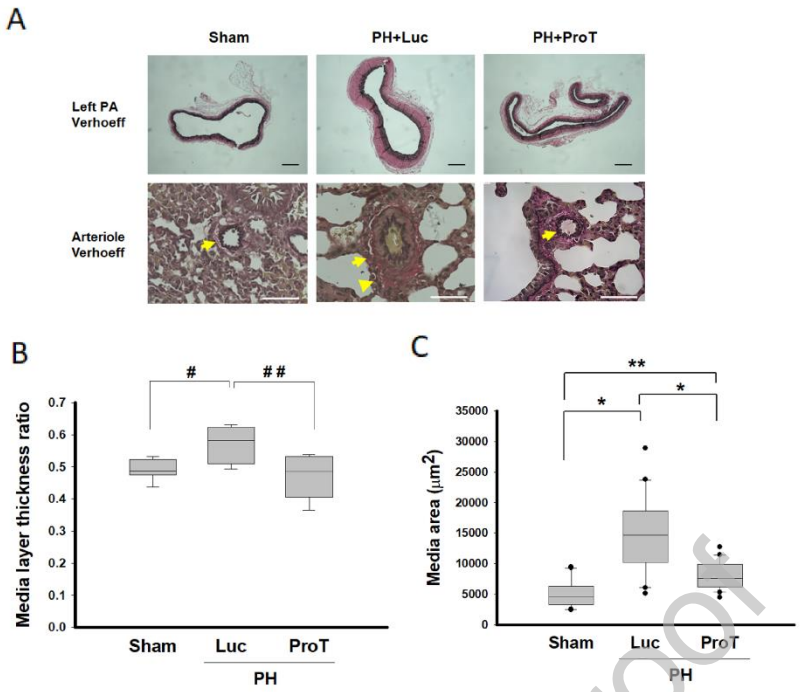

Figure 3. Histological remodeling of pulmonary arteries (PAs) and arterioles in flow-induced pulmonary hypertension (PH). **A.** Representative Verhoeff's stain for media layer of PA (upper panel; ×40 magnification, scale bar corresponds to 200 μm) and pulmonary intra-acinar arterioles with diameter < 100 μm (yellow arrow in lower panel; yellow arrow head indicates perivascular plexiform formation; ×400 magnification, scale bar corresponds to 50 μm). **B.** Summary of the media layer thickness ratio data ($^{\#}P = 0.045$; $^{\#\#}P = 0.034$ using post-hoc Holm–Sidak method; ten counts for each section, three sections for each rat PA; n = 4–6 per group). **C.** Quantitative analysis of the media area. ($^{*}P < 0.001$; $^{**}P = 0.015$ using post-hoc Dunn's method; nine counts for each rat with 5 rats/group).. Luc: luciferase gene delivery; ProT: prothymosin α gene delivery.

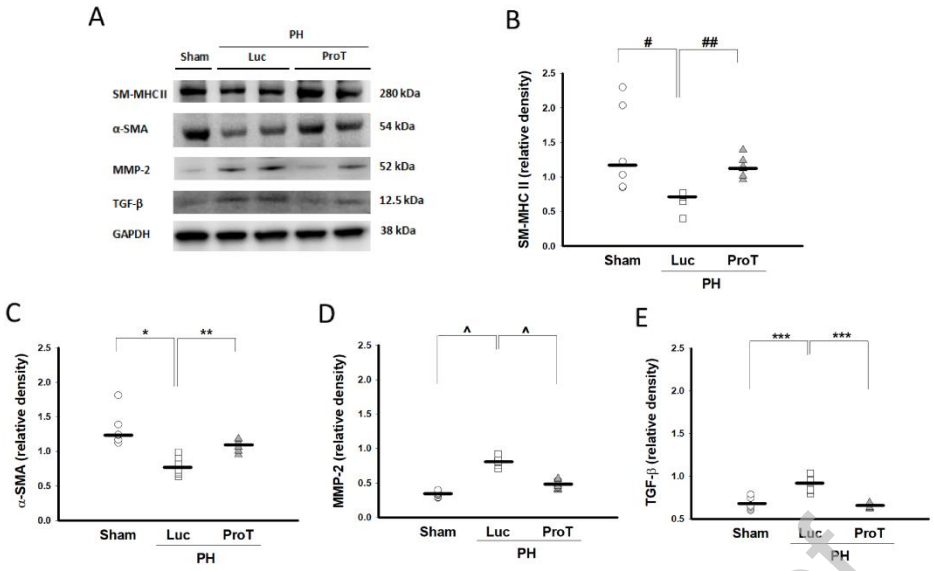

Figure 4. Pulmonary artery vascular smooth muscle cell phenotype shifting in flow-induced pulmonary hypertension (PH). **A.** Representative immunoblots of α-smooth muscle actin (SMA), smooth muscle myosin heavy chain (SM-MHC) class II, matrix metalloproteinase (MMP)-2, and transforming growth factor (TGF)-β. **B.** Quantitative analysis for SM-MHC II, **C.** α-SMA, **D.** MMP-2, and **E.** TGF-β. $^{\#}P = 0.005$, $^{\#\#}P = 0.003$, $^{*}P < 0.001$, $^{**}P = 0.033$, and $^{***}P = 0.004$ using post-hoc Dunn's method, $^{\wedge}P < 0.001$ using post-hoc Holm–Sidak method, n = 6–7/group. PH: pulmonary hypertension. Luc: luciferase gene delivery. ProT: prothymosin-α gene delivery. GAPDH: Glyceraldehyde-3-Phosphate Dehydrogenase. Da: Dalton. The horizontal lines in **B, C, D, and E.** denote the median value.

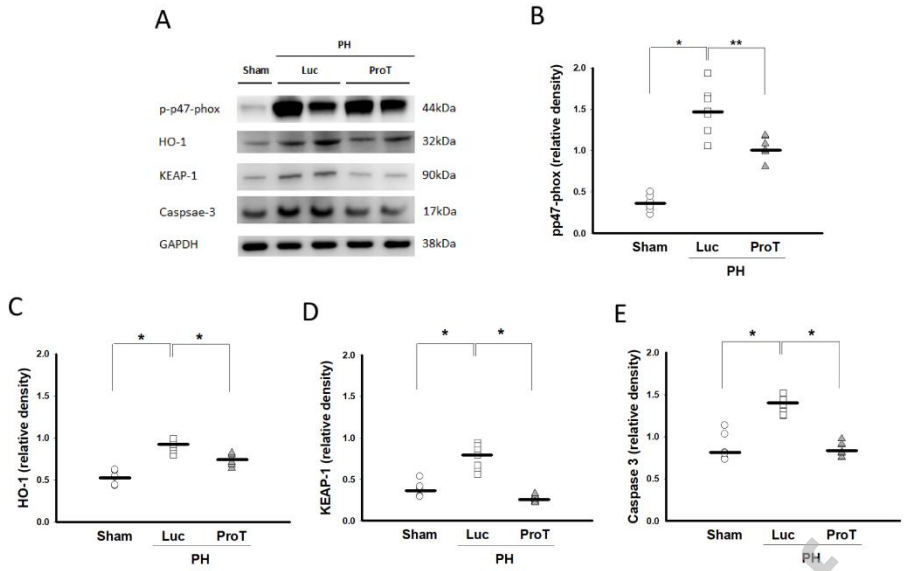

Figure 5. Changes in oxidative stress in pulmonary arteries (PAs). **A**. Representative immunoblotting for phosphorylated (p) p47-phox, heme oxygenase (HO)-1, Kelch-like ECH-associated protein (KEAP)-1, and caspase-3. Quantitative analysis for **B**. pp47-phox, **C**. HO-1, **D**. KEAP-1, and **E**. Caspase 3 (**P* < 0.001; ***P* = 0.001, using post-hoc Tukey test; n = 6–7 per group). PH: pulmonary hypertension. Luc: luciferase gene delivery. ProT: Prothymosin α gene delivery. GAPDH: Glyceraldehyde-3-Phosphate Dehydrogenase. Da: Dalton. The horizontal lines in **B, C, D, and E.** denote the median value.

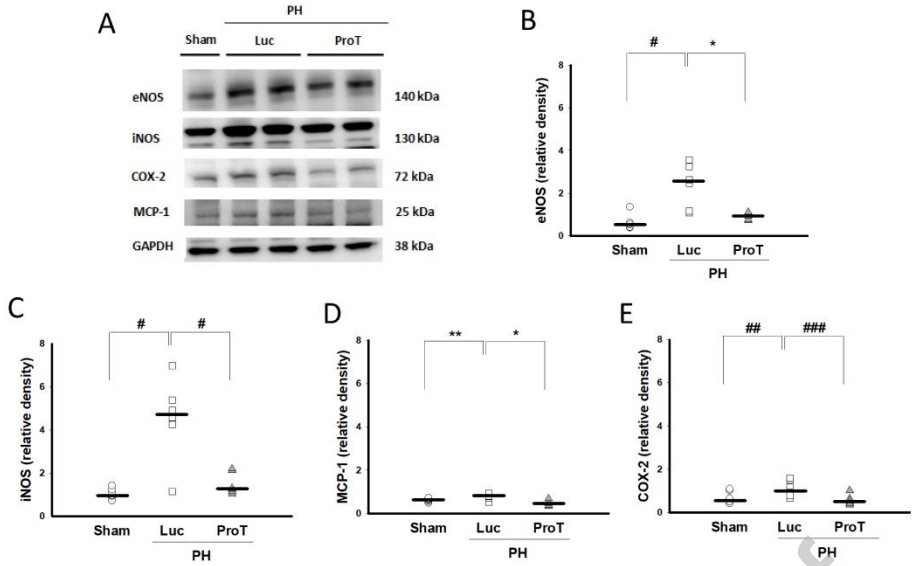

Figure 6. Inflammation markers in pulmonary arteries of pulmonary hypertension (PH) rats luciferase (Luc) or prothymosin α (*ProT*) gene transduction. **A**. Representative immunoblotting for endothelial nitric oxide synthase (eNOS), inducible nitric oxide synthase (iNOS), cyclooxygenase (COX)-2, and monocyte chemoattractant protein (MCP)-1. Quantitative analysis for **B**. eNOS, **C**. iNOS, **D**. COX-2, and **E**. MCP-1. ($^{\#}P < 0.001$; $^{*}P = 0.003$; $^{**}P = 0.025$; $^{\#\#}P = 0.012$; $^{\#\#\#}P = 0.002$ using post-hoc Tukey test; n=6–7 per group). GAPDH: Glyceraldehyde-3-Phosphate Dehydrogenase. Da: Dalton. The horizontal lines in **B, C, D, and E.** denote the median value.

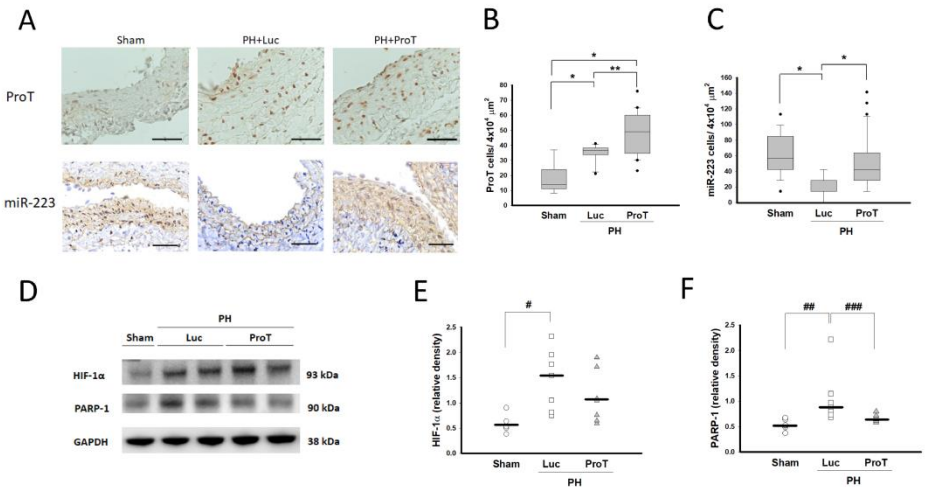

Figure 7. Tissue expressions of prothymosin α (ProT), poly(ADP-ribose)polymerase (PARP)-1, and hypoxia inducible factor (HIF)-1α in main pulmonary arteries (PAs). **A**. Immunohistochemistry of ProT and miR-223. **B**. Quantitative plot of ProT (+) cells per 40000 µm^2 (*P <.0.001; **P = 0.006 using post-hoc Holm–Sidak method; each PA was examined in five different sections with five counts for each section, a total of 25 counts per rat and 5 rats/group; ×400 magnification). Scale bar corresponds to 50 µm. **C**. Quantitative plot of miR-223 (+) cells per 40000 µm^2 (*P < 0.001 using post-hoc Dunn's method; each PA was examined in three different sections with five counts for each section, a total of 15 counts per rat and 3 rats/group; ×400 magnification). Scale bar corresponds to 30 µm. **D**. Representative immunoblotting for HIF-1α and PARP-1. Quantitative analysis for **E**. HIF-1α and **F**. PARP-1 ($^{\#}P$ = 0.013, $^{\#\#}P$ < 0.001, $^{\#\#\#}P$ = 0.043 using post-hoc Dunn's method; n = 6–7 per group). PH: pulmonary hypertension. GAPDH: Glyceraldehyde-3-Phosphate Dehydrogenase. Da: Dalton. The horizontal lines in **B**, **C, E, and F** denote the median value.

Table 1. Echocardiographic measurements

Variables	Sham (n = 7)	PH+*Luc* (n = 6)	PH+*ProT* (n = 6)	*P* value
Main Pulmonary artery diameter (mm)	3.19 ± 0.57	5.64 ± 0.78*	4.46 ± 0.61	< 0.001
Pulmonary artery peak flow velocity (cm/s)	63.85 ± 7.72	92.00 ± 11.47**	74.40 ± 7.96	< 0.001
Right ventricle diameter (mm)	4.21 ± 0.22	7.38 ± 1.18‡	6.00 ± 0.90	< 0.001
Tricuspid peak flow velocity (cm/s)	70.70 ± 11.68†	107.80 ± 12.64	94.00 ± 17.51	0.002
Left ventricle ejection fraction (%)	65.71 ± 9.87	62.58 ± 3.55	59.91 ± 7.62	0.467

Holm–Sidak method was used for post-hoc analysis. *Luc*: luciferase gene delivery. *ProT*: Prothymosin α gene delivery. Data are presented as mean ±SD.

**P* = 0.011 vs PH+*ProT*; *P*<0.001 vs sham

***P* = 0.014 vs PH+*ProT*; *P*<0.001 vs sham

‡*P* = 0.005 vs PH+*ProT*; *P*<0.001 vs sham

†*P* = 0.002 vs PH+*Luc*, and *P*=0.033 vs PH+*ProT*; *P*=0.143 for PH vs PH+*ProT*.

Graphical Abstract